

Cell Motion Alignment as Polarity Memory Effect

Katsuyoshi Matsushita*, Kazuya Horibe, Naoya Kamamoto and Koichi Fujimoto

Department of Biological Sciences, Osaka University, Toyonaka, Osaka, Japan

July 26, 2019

Abstract

The clarification of the motion alignment mechanism in collective cell migration is an important issue commonly in physics and biology. In analogy with the self-propelled disk, the polarity memory effect of eukaryotic cell is a fundamental candidate for this alignment mechanism. In the present paper, we theoretically examine the polarity memory effect for the motion alignment of cells on the basis of the cellular Potts model. We show that the polarity memory effect can align motion of cells. We also find that the polarity memory effect emerges for the persistent length of cell trajectories longer than average cell-cell distance.

Motion alignment plays various roles widely in self-propelled systems including migrating cells[1], moving organisms [2], molecular motors[3], self-propelled droplets [4] and swarming robots [5]. In particular, the alignment of migrating cells is indispensable for cell organizing in organogenesis, wound healing and immune response [6, 7, 8]. In these processes, migrating cells exhibit collective behavior commonly observed in self-propelled systems [9, 10, 11], including various patterns [12, 13], active turbulence [14], traveling wave excitation [15]. For the understanding of these behavior, an important issue is to clarify the alignment mechanism as their underlying basis.

The alignment mechanisms of other self-propelled systems may give hints for this clarification. In many self-propelled systems including bird flocking [16, 17], the direct aligning-interaction through visual contact is sup-

posed and is expressed as an interaction between vector degrees of freedom, which are so-called polarity. Unfortunately, this direct aligning-interaction is not expected in migrating cells lacking visual contact. As another candidate, the peculiar alignment of self-propelled disks or deformable particles is considerable[18, 19, 20, 21] because it requires only an indirect interaction of polarities through excluded volume. In these cases, the direct aligning-interaction is not necessary at least for this alignment. Especially for the disks, the polarity memory recording the past motion aligns the subsequent motion through collisions even with rotation-symmetric excluded volume [22, 23, 24, 25].

Since the polarity memory recording cell motion is well known for eukaryotic cells[26, 27], the polarity memory effect is expected to work in the collective cell migration of *Dictyostelium Discoideum* (Dicty)[28, 29], keratocytes[30, 31] and neural crest cell[32]. In the studies of these collective migration [33, 34], since the alignment was attributed only to the chemotaxis[35, 36], the contribution of polarity memory has been overlooked. In addition, even when the chemotaxis is artificially inhibited [37, 15], other effects including intercellular adhesion [38, 39], shape anisotropy[40, 41, 42] or contact inhibition[43, 44]/activation[45, 46] of locomotion have the polarity memory effect be experimentally invisible. Therefore, the theoretical examination to evaluate the polarity memory effect is a powerful method to clarify the alignment mechanism.

In this examination, the spontaneous fluctuation in the shape may give considerable differences between eukaryotic cells and self-propelled disks [47, 48], even when the averaged cell shape is rotation symmetric. In particular,

*kmatsu@cp.cmc.osaka-u.ac.jp

since the shape fluctuation due to protrusion [49, 50] or blebbing [51, 52] stochastically propels cells, the fluctuation clearly gives the qualitative difference between cells and self-propelled disks in the propulsion mechanism. In fact, the behavior of the cells cannot directly be deduced from the theory of the self-propelled disks, because cells lose propulsion in unfluctuating shape like the disks. Therefore, for the theoretical examination, the theory, only by itself, is insufficient. At least, it should be combined with the cellular model suitably expressing the propulsion mechanism[53].

In the present work, we investigate a model for migrating cells with the polarity memory and the interaction only through rotation-symmetric excluded volume. We perform Monte Carlo simulations based on the Cellular Potts model[54, 55] and thereby confirm that the alignment mechanism due to the polarity memory is effective. Then, we further examine the shape fluctuation effect on the alignment and show that the alignment emerges at the crossover between the persistent length of cell trajectories and the average cell-cell distance when the propulsion is stronger than the shape fluctuation.

Let us consider the two dimensional Cellular Potts model consisting of migrating cells with the polarity memory [56]. This model is defined by the Hamiltonian,

$$\mathcal{H} = \mathcal{H}_{\text{CC}} + \mathcal{H}_{\text{CE}} + \mathcal{H}_{\text{Vol}} + \mathcal{H}_{\text{Mot}} \quad (1)$$

for given Potts state $\{m(\mathbf{r})\}$ on the square lattice. Here, \mathbf{r} represents a site in the square lattice. $m(\mathbf{r})$ takes a number from 0 to the number of cells N . $m(\mathbf{r}) = 0$ expresses that the site \mathbf{r} is empty. Otherwise, $m(\mathbf{r})$ is the index of cells on the site \mathbf{r} . For simplicity of examination, we fix N .

The first and second terms in rhs of Eq. (1),

$$\mathcal{H}_{\text{CC}} = \Gamma \sum_{\langle \mathbf{r}\mathbf{r}' \rangle} \eta_{m(\mathbf{r})m(\mathbf{r}')} \eta_{0m(\mathbf{r}')}\eta_{m(\mathbf{r})0}, \quad (2)$$

$$\mathcal{H}_{\text{CE}} = \Gamma_0 \sum_{\langle \mathbf{r}\mathbf{r}' \rangle} (\delta_{m(\mathbf{r})0}\eta_{0m(\mathbf{r}')} + \eta_{m(\mathbf{r})0}\delta_{m(\mathbf{r}')0}), \quad (3)$$

represent interface parts of cell-cell and cell-empty space. δ_{mn} is Kronecker δ and η_{mn} is defined by $(1 - \delta_{mn})$. Γ represents cell-cell interface tension and Γ_0 cell-empty space interface tension. For $\Gamma > 2\Gamma_0$ [57], cells are suspended. Since the suspended cells interact only with excluded volume, we impose this condition on Γ for our purpose. The summations in rhs of these equations are taken over all

the neighboring sets which consist of the nearest and next nearest neighbor sites[54].

The third term in the rhs of Eq. (1),

$$\mathcal{H}_{\text{Vol}} = \kappa \sum_{m=1}^N \left(1 - \frac{\sum_{\mathbf{r}} \delta_{mm(\mathbf{r})}}{V} \right)^2. \quad (4)$$

represents the bulk part. This term expresses the situation where the occupation area of cells is maintained to be V , as empirically observed. Here, κ represents area stiffness.

The fourth term in the rhs of Eq. (1),

$$\mathcal{H}_{\text{Mot}} = -\varepsilon \sum_{m=1}^N \sum_{\mathbf{r}} \delta_{mm(\mathbf{r})} \mathbf{p}_m \cdot \mathbf{e}_m(\mathbf{r}), \quad (5)$$

represents propulsion [56]. Here, ε is the strength of propulsion, \mathbf{p}_m is the unit vector of the polarity and $\mathbf{e}_m(\mathbf{r})$ is the unit vector indicating from the center of the m -th cell $\mathbf{R}_m = \sum_{\mathbf{r}} \mathbf{r} \delta_{mm(\mathbf{r})} / \sum_{\mathbf{r}} \delta_{mm(\mathbf{r})}$ to a site \mathbf{r} . Notice that the cell takes rotation-symmetric shape even with this term, because this term does not induce tensile stress. \mathbf{p}_m obeys [30, 58]

$$\frac{d\mathbf{p}_m}{dt} = \frac{1}{a\tau_p\Delta t} \left[\frac{d\mathbf{R}_m}{dt} - \left(\mathbf{p}_m \cdot \frac{d\mathbf{R}_m}{dt} \right) \mathbf{p}_m \right]. \quad (6)$$

Here, t is time, τ_p is the time scale ratio of \mathbf{p}_m change to \mathbf{R}_m change and a is the lattice constant. This equation represents the polarity memory during the time of $\tau_p\Delta t$ in the sense of the solution, $\mathbf{p}_m(t) \sim \int_{-\infty}^t dt' d\mathbf{R}_m(t')/dt' \exp[-(t-t')/\tau_p\Delta t]/a\tau_p\Delta t$ [56]. Here, Δt represents the time of single monte carlo steps (mcs) and we set $\Delta t = 1$ for simplicity.

On the basis of \mathcal{H} , the shape fluctuation of cells is reproduced by monte carlo simulation [53]. In this simulation, the state $\{m(\mathbf{r})\}$ is updated to $\{m'(\mathbf{r})\}$ as follows: firstly a site \mathbf{r} is randomly selected. Then, the state $m(\mathbf{r}')$ at a randomly selected site \mathbf{r}' in its neighboring set is copied to the site \mathbf{r} . This copy is accepted with the Metropolis probability $P(m'(\mathbf{r})|m(\mathbf{r})) = \min(1, \exp\{-\beta[\mathcal{H}(m(\mathbf{r})) - \mathcal{H}(m'(\mathbf{r}))]\})$, where β is inverse temperature. Otherwise, this copy is rejected. We call this procedure a copy trial. Mcs conventionally consist of $16L^2$ copy trials [54], where L is the linear size of square system. The series of mcs expresses the shape fluctuation. For each mcs, \mathbf{p}_m is assumed to be a slow variable

with \mathbf{R}_m and is updated once by the Euler method [58]. Simultaneously, \mathbf{R}_m is also updated and is fixed in mcs.

In this simulation, we employ the following parameters: L is 256 and V is 64. These parameters are chosen so as to realize the suspended state for the tractable N from 64 to 512. These N corresponds to the area fraction of ϕ from 0.11 to 0.85. Additionally for the same purpose, we choose surface tensions $\Gamma = 6.0$ and $\Gamma_0 = 1.0$. To consider highly fluctuated cells in their shape, we consider low value of inverse temperature β of 0.3. Since $\beta \geq 0.3$ avoids cell fragmentation, this value supports both high fluctuation and stable cells.

By simulating cell dynamics in this model, we examine this model cell for the polarity memory effect. Firstly, we decide the simulation strategy on the basis of the theory of the self-propelled disk. To the theory, the motion alignment appears only in the low damping parameter γ for the angle of \mathbf{p}_m , θ_m . Therefore, when the polarity memory effect works, the alignment depends on γ in the same manner with the disk and a certain threshold γ_c for the alignment is present. By the reproduction of this dependence, we evaluate the polarity memory effect.

In order to determine γ , let us derive an effective self-propelled disk from this model. Since γ is independent of intercellular interaction, we consider an isolated cell for simplicity and ignore the intercellular interaction. In our overdamped simulation based on \mathcal{H} , we can suppose the Langevin equation of cell motion,

$$\frac{d\mathbf{R}_m}{dt} = \varepsilon \mathbf{p}_m \cdot \sum_r \delta_{mm(r)} \left\langle \frac{\partial \mathbf{e}_m(\mathbf{r})}{\partial \mathbf{r}} \right\rangle_{\mathbf{R}_m} + \mathbf{f} \quad (7)$$

In the derivation of force in rhs, we use the fact that \mathcal{H}_{Mot} is only the term explicitly depending on \mathbf{R}_m in \mathcal{H} . We also interpret the \mathbf{R}_m derivative as the derivative of the cell boundary coordinate \mathbf{r} with fixed \mathbf{R}_m . This is because the force is practically exerted on the cell boundary as defined in the virtual work due to the deformation of cell shape. We divide this force into the shape-average and -fluctuation parts, where $\langle \dots \rangle_{\mathbf{R}_m}$ represents the average over cell shapes with fixed \mathbf{R}_m and \mathbf{f} is deviation representing the shape fluctuation of cells. In addition, we reformulate the equation of \mathbf{p}_m in Eq. (6) as an equation of θ_m similar to the self-propelled disk [23]. For this purpose, we substitute \mathbf{p}_m with $(\cos \theta_m, \sin \theta_m)$ and $d\mathbf{R}_m/dt$ with $|d\mathbf{R}_m/dt|(\cos \psi_m, \sin \psi_m)$, where ψ_m is the angle of

the cell velocity. Then, by multiplying $d\mathbf{R}_m/dt$ to both sides of Eq. (6), we read

$$\frac{d\theta_m}{dt} = -\frac{1}{a\tau_p} \left| \frac{d\mathbf{R}_m}{dt} \right| \sin(\theta_m - \psi_m). \quad (8)$$

The former, Eq. (7) is identical to an overdamped active Brownian particle [25] rather than the self-propelled disk [22, 23] in the sense of similarity in overdamping feature. In contrast, the latter, Eq. (8) is similar to the self-propelled disk. In the comparison of Eq. (8) with the corresponding equation in the literature [23], $|d\mathbf{R}/dt|/a\tau_p$ is read as γ .

In the self-propelled disk, the damping parameter γ is a control parameter of the motion alignment [22, 23]. Naively, the dependence on $\gamma = |d\mathbf{R}/dt|/a\tau_p$ in our model is evaluable from the τ_p dependence. However, in contrast to self-propelled disk, γ also depends on the cell velocity, $|d\mathbf{R}/dt|$, which is not a model parameter. To consider this effect, we focus on the dependence of the alignment not only on τ_p and but also ε . Here, ε is one of the parameters which determine $|d\mathbf{R}/dt|$ in Eq. (7) and the dependence of $|d\mathbf{R}/dt|$ on ε is $|d\mathbf{R}/dt| \sim \varepsilon$ for ε larger than \mathbf{f} .

Secondarily, we give the method to identify the motion alignment in our examination. Refer to the previous work[17, 23], we define the motion alignment by finite values of the order parameter of \mathbf{p}_m ,

$$P = \left| \frac{1}{T} \int_{T_0}^{T+T_0} dt \frac{1}{N} \sum_{m=1}^N \mathbf{p}_m \right|. \quad (9)$$

Here, T_0 represents the number of mcs for the relaxation to the steady state. T is the number of mcs for the time average. We empirically employ $T_0 = 10^6$ mcs and $T = 10^5$ mcs [58]. Here, note that P is not adequate for detection of heterogeneous alignments of motion, including vortexes. Therefore, to avoid the heterogeneous alignments due to the boundary effect of the system, we simply employ the periodic boundary condition.

To examine the dependence of the alignment on τ_p and ε , we calculate P as a function of τ_p for various ε . For easily observing the alignment, we choose relatively high area fraction of cells $\phi = NV/L^2 \approx 0.43$. The data are plotted in Fig. 1(a). P at $\tau_p = 0$ is almost 0 over all ε . In this case, the cells randomly move and \mathbf{p}_m does not align as shown in Fig. 1(b). With increasing τ_p , P is kept to

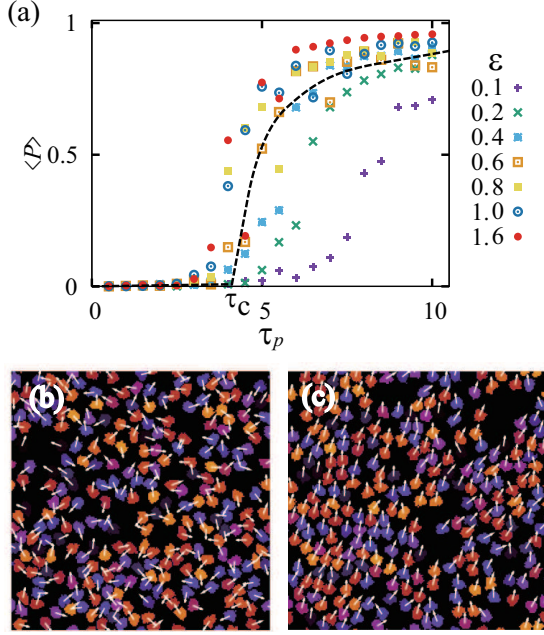


Figure 1: (a) $\langle P \rangle$ as a function of time scale ratio τ_p in Eq. (6) for various strength of motility ε . The different symbols indicate different values of ε . Snapshots for (b) $\varepsilon=1.0$ and $\tau_p=1.0$, and for (c) $\varepsilon=1.0$ and $\tau_p=10.0$. Different color region indicates different Potts domains, namely cells. Black region represents the empty region. White arrows represent the direction of polarity.

be 0 for small τ_p and then rapidly increases at a threshold value of τ_p , τ_c , excepting $\varepsilon = 0.1$, where the alignment is unstable. After this increasing, P takes high values around unity which indicates the motion alignment shown in Fig. 1(c). Therefore, even in cells propelled by shape fluctuation, the polarity memory effect works, excepting cases of too small ε 's.

In addition, τ_c is almost independent of ε excepting too small value. This independence seemingly contradicts the expectation from the constant threshold $\gamma_c = |d\mathbf{R}/dt|/a\tau_c$ in previous work [23]. In fact, in the linear response $|d\mathbf{R}_m/dt| \sim \varepsilon$, the expectation of $\tau_c \sim \varepsilon$ is not shown in Fig. 1(a). Since the constant threshold γ_c , which leads to this contradiction, is based on the theory of rigid self-propelled disk, the rigidity of the disk is a candidate origin

of this contradiction. Therefore, to understand this independence, the shape fluctuation of cells should be considered beyond the theory for the rigid disk.

To explore the origin of this independence, we consider the effect of this shape fluctuation in the motion alignment. This effect comes from \mathbf{f} in Eq. (7) and reduces the polarity memory effect, through $|d\mathbf{R}_m/dt|$ and ψ_m in Eq. (8). Intercollision processes reflect this reducing because it shortens the persistent length of cell trajectories, l_p , which is defined for an isolated cell differently from the mean free path. Since the intercollision processes also reflect the cell density ϕ , changes of ϕ interferes the effect of l_p . Therefore, by utilizing this interference in the intercollision processes, we can evaluate the shape fluctuation effect.

For this evaluation, we calculate P as a function of τ_p for various values of ϕ with $\varepsilon = 1.0$ ($\gg f$). The result of P is plotted as a function of τ_p for various ϕ in Fig. 2. P commonly takes 0 for small τ_p and increases with increasing τ_p . The alignment threshold, τ_c , where P rapidly increases, largely decreases with increasing ϕ in contrast to the independence on ε in Fig. 1(a).

Let us consider the mechanism of this strong decreasing τ_c with increasing ϕ . From discussions so far, we focus on intercollision processes. In these processes, since p_m depends on \mathbf{f} through $|d\mathbf{R}_m/dt|$ in Eqs. (7) and (8), cells must maintain their direction of polarity against the disorder of shape fluctuation for the stable alignment. Therefore, the persistent length, l_p , exists as a finite value and determines the stability of alignments. This situation is contrast to the self-propelled disks having infinite l_p due to rigid shape[23]. Hence, for migrating cells, τ_c is determined not only by γ but also by l_p . In small shape fluctuation, the memory time of polarity is typically given almost by $t_R = \gamma^{-1} = a\tau_p|d\mathbf{R}_m/dt|^{-1}$. This time gives the persistent length,

$$l_p \simeq t_R \left| \frac{d\mathbf{R}_m}{dt} \right| = a\tau_p. \quad (10)$$

l_p must be larger than the intercellular distance l_d for cells to maintain the direction of motion during intercollision processes. This gives a necessary condition for the alignment, namely, $l_p > l_d$.

To intuitively understand this condition, we discuss the two serial collision processes shown in Figs. 3(a) and 3(b). Firstly, we consider the case of $l_p > l_d$. In this case,

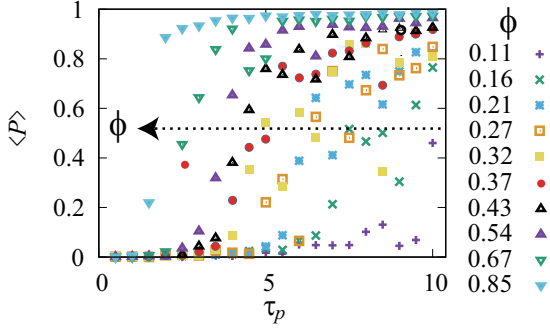


Figure 2: $\langle P \rangle$ as a function of time scale ratio τ_p in Eq. (6) for various area fraction ϕ . Different symbols indicate different value of ϕ . The arrow shows the decreasing of τ_c with increasing ϕ .

as shown in Fig. 3(a), the direction of motion after the 1st collision is maintained until the 2nd collision, because the 2nd collision typically occurs in the cell movement length of l_d . Owing to the polarity memory effect, cells align their motion in the common direction through the 1st and 2nd collisions[22, 23]. This aligning repeats in the following collisions and finally results in the motion alignment over all cells. Next, we consider the other case of $l_p < l_d$. In this case, the polarity relaxes owing to the shape fluctuation in the intercollision periods. Therefore, as shown in Fig. 3(b), even when the motion of cells temporarily align in the same direction in the 1st collision, then the aligned direction of motion is lost until the 2nd collision. As a result, the motion alignment does not growth over all cells and thereby cannot induces the motion alignment over all cells. The marginal case between these cases, $l_p \approx l_d$, determines τ_c .

On the basis of this marginal condition, we can discuss the independence of τ_c on ε in Fig. 1(a). For this discussion, notice that since this system corresponds to the active Brownian particle with high rotational Peclet number limit because of the absence of heat bath in Eq. (8) [25], the phase separation does not appear. Therefore, the configuration of cells becomes uniform (See Figs. 1(b) and 1(c)) and thereby l_d is typically $a\phi^{-1/d}$. Here, $d = 2$ is the dimension of space. Hence, since $l_d = a\phi^{-1/d}$ and l_p in Eq. (10) are commonly independent of $d\mathbf{R}_m/dt$, the marginal condition is also independent of $d\mathbf{R}_m/dt$. This is

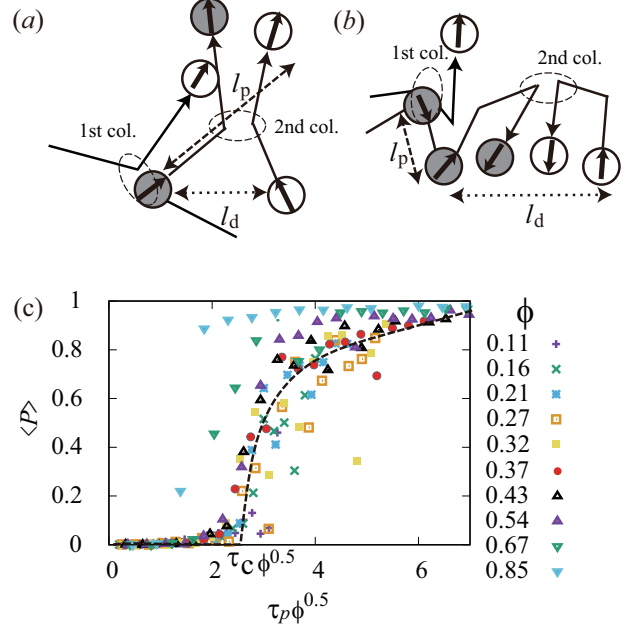


Figure 3: Schematic view of two sequential collision process of cells (grey circle) for (a) $l_p > l_d$ and for (b) $l_p < l_d$. The circles represent a cell and intracircle arrows represent a polarity direction. Solid arrows indicates the cell motion and their straight regions almost correspond to shorter one in l_d and l_p . Dashed and dotted lines with arrow heads represent l_p and l_d . (c) $\langle P \rangle$ as a function of $\tau_p \phi^{1/d}$. Different symbols indicate different value of ϕ .

the origin of the independence of τ_c on ε .

To confirm this condition, we can use the fact that $l_p/a = \tau_c$ must be equal to $l_d/a = \phi^{-1/d}$. In this case, τ_c decreases with increasing ϕ as keeping the value of $l_p/l_d = \tau_c \phi^{1/d}$. In Fig. 3(c), we replot P in Fig. 2 as a function of $\tau_p \phi^{1/d}$. In comparison with data in Fig. 2, the data collapse into a single curve, excepting the cases of high area fractions $\phi = 0.67$ and $\phi = 0.85$ with crowding effects [59, 60]. This result suggests that the crossover of length scales between the persistent length, l_p , and intercellular distance, l_d , determines τ_c .

In conclusion, similarly to the self-propelled disks, cells align their motion by a pure polarity memory effect, while the condition for alignment has a slight correction

due to the shape fluctuation[61]. The polarity effect is a powerful candidate of the alignment mechanism comparably with the shape-velocity coupling effect for the soft deformable particles [62, 20, 21]. This implies the biological function of the polarity memory as the driving force of the motion alignment. A prominent example is the early development stage of Dicty [63] and therein Dicty exhibits the extension of memory time [28]. For utilizing this function in motion alignment, Dicty may strategically extend the memory time of polarity in this early stage.

We thank fruitful discussions with H. Kuwayama, H. Hashimura, S. Yabunaka, K. Hironaka, T. Hiraoka and R. Ishiwata. We also thank the support on the research resource by M. Kikuchi and H. Yoshino. This work is supported by supported by JSPS KAKENHI (Grant Number 19K03770).

References

- [1] *Cell Migration: Signalling and Mechanisms*, ed. F. Entschladen and K. S. Zanker (S Karger Pub, 2009).
- [2] T. Vicsek and A. Zafeiris: *Phys. Rep.* **517** (2012) 71.
- [3] V. Schaller, C. Weber, C. Semmrich, E. Frey, and A. R. Bausch: *Nature* **467** (2010) 73.
- [4] R. Seemann, J.-B. Fleury, and C. C. Maass: *Eur. Phys. J.* **225** (2016) 2227.
- [5] M. Brambilla, E. Ferrante, M. Birattari, and M. Dorigo: *Swarm Intell.* **7** (2013) 1.
- [6] C. J. Weijer: *J. Cell Sci.* **122** (2015) 3215.
- [7] P. Friedl and D. Gilmour: *Nat. Rev. Mol. Cell Biol.* **10** (2009) 445.
- [8] P. Rørth: *Annu. Rev. Cell Dev. Biol.* **25** (2009) 407.
- [9] P. Romanczuk, M. Br. W. Ebeling, B. Lindner, and L. Schimansky-Geier: *Eur. Phys. J.* **202** (2012) 1.
- [10] M. C. Marchetti, J. F. Joanny, S. Ramaswamy, T. B. Liverpool, J. Prost, M. Rao, and R. A. Simha: *Rev. Mod. Phys.* **85** (2013) 1143.
- [11] A. Doostmohammadi, J. Igns-Mullol, J. M. Yeomans, and F. Sagués: *Nat. Comm.* **9** (2018) 3246.
- [12] J.-I. Wakita, S. Tsukamoto, K. Yamamoto, M. Katori, and Y. Yamada: *J. Phys. Soc. Jpn.* **84** (2015) 124001.
- [13] K. Kawaguchi, R. Kageyama, and M. Sano: *Nature* **545** (2017) 327.
- [14] H. H. Wensink, J. Dunkel, S. Heidenreich, K. Drescher, R. E. Goldstein, H. Löwen, and J. M. Yeomans: *Proc. Natl. Acad. Sci. USA* **109** (2012) 14308.
- [15] H. Kuwayama and S. Ishida: *Sci. Rep.* **3** (2013) 2272.
- [16] C. W. Reynolds: *Computer Graphics* **21** (1987) 25.
- [17] T. Vicsek, A. Czirók, E. Ben-Jacob, I. Cohen, and O. Shochet: *Phys. Rev. Lett.* **75** (1995) 1226-1229.
- [18] C. A. Weber, T. Hanke, J. Deseigne, S. Léonard, O. Dauchot, E. Frey, and H. Chaté: *Phys. Rev. Lett.* **110** (2013) 208001.
- [19] K.-D. N. T. Lam, M. Schindler, and O. Dauchot: *New J. Phys.* **17** (2015) 113056.
- [20] S. Yamanaka and T. Ohta: *Phys. Rev. E* **90** (2014) 042927.
- [21] T. Ohta: *J. Phys. Soc. Jpn.* **86** (2017) 072001.
- [22] T. Hanke, C. A. Weber, and E. Frey: *Phys. Rev. E* **88** (2013) 052309.
- [23] T. Hiraoka, T. Shimada, and N. Ito: *Physical Review E* **94** (2016) 062612.
- [24] T. Hiraoka, T. Shimada, and N. Ito: *Journal of Physics: Conference Series* **921** (2017) 012006.
- [25] A. Martín-Gómez, D. Levis, A. D'áz-Guilera, and I. Pagonabarraga: *Soft Matter* **14** (2018) 2610.
- [26] R. J. Petrie, A. D. Doyle, and K. M. Yamada: *Nature Rev. Mol. Cell Biol.* **10** (2009) 538.

- [27] X. Trepap and E. Sahai: *Nat. Phys.* **14** (2018) 671.
- [28] H. Takagi, M. J. Sato, T. Yanagida, and M. Ueda: *PLOS One* **3** (2008) e2648.
- [29] L. Li, E. C. Cox, and H. Flyvbjerg: *Phys. Biol.* **8** (2011) 046006.
- [30] B. Szabó, G. J. Szollosi, B. Gonci, Z. Juranyi, D. Selmecki, and T. Vicsek: *Phys. Rev. E* **74** (2006) 061908.
- [31] A. F. M. Marée, A. Jilkine, A. Dawes, Verónica, A. Grieneisen, and L. Edelstein-Keshet: *Bull. Math. Biol.* **68** (2006) 1169.
- [32] A. Szabó, M. Melchionda, G. Nastasi, M. L. Woods, S. Campo, R. Perris, and R. Mayor: *J. Cell Biol.* **215** (2016) 543.
- [33] E. Méhes and T. Vicsek: *Comput. Adapt. Syst. Mod.* **1** (2013) 4.
- [34] A. Haeger, K. Wolf, M. M. Zegers, and P. Friedl: *Trends Cell Biol.* **25** (2015) 556.
- [35] A. Bagorda and C. A. Parent: *J. Cell Sci.* **121** (2008) 2621.
- [36] M. Akiyama, T. Sushida, S. Ishida, and H. Haga: *Develop. Growth Differ.* **59** (2017) 471.
- [37] H. Kuwayama, S. Ishida, and P. J. M. V. Haastert: *J. Cell Biol.* **123** (1993) 1453.
- [38] O. Iilina and P. Friedl: *J. Cell Sci.* **122** (2009) 3203.
- [39] K. Matsushita: *Phys. Rev. E* **97** (2018) 042413.
- [40] R. M. Merks, S. V. Brodsky, M. S. Goligorsky, S. A. Newman, and J. A. Glazier: *Develop. Biol.* **289** (2006) 44.
- [41] J. S. T. Bley, L. Søggaard-Andersen, and A. Deutsch: *J. Stat. Phys.* **128**, (2007) 269.
- [42] T. Hirashima, E. G. Rens, and R. M. H. Merks: *Development, growth & differentiation* **59** (2017) 329.
- [43] R. Mayor and C. Carmona-Fontaine: *Trends Cell Biol.* **20** (2010) 319.
- [44] S. K. Schnyder, J. J. Molina, Y. Tanaka, and R. Yamamoto: *Sci Rep.* **7** (2017) 5163.
- [45] T. Fujimori, A. Nakajima, N. Shimada, and S. Sawai: *Proc.* **116** (2019) 4291.
- [46] T. Hiraiwa: *Phys. Rev. E* **99** (2019) 012614.
- [47] G. B. Blanchard, S. Murugesu, R. J. Adams, A. Martínez-Arias, and N. Gorfinkiel: *Development* **137** (2010) 2743.
- [48] A. Muñoz, D. A. Fletcher, and O. D. Weiner: *Trends in Cell Biology* **23** (2013) 47.
- [49] L. P. Bignold: *Experientia* **43** (1987) 860.
- [50] P. J. M. V. Haastert: *Sci. Signal.* **4** (2011) pe6.
- [51] O. T. Fackler and R. Grosse: *J. Cell. Biol.* **181** (2008) 879.
- [52] G. Charras and E. Paluch: *Nature Rev. Mol. Cell Biol.* **9** (2008) 730.
- [53] A. R. A. Anderson, M. A. J. Chaplain, and K. A. Rejniak: *Single-Cell-Based Models in Biology and Medicine* (Birkhauser Verlag AG, Basel, 2007).
- [54] F. Graner and J. A. Glazier: *Phys. Rev. Lett.* **69** (1992) 2013.
- [55] F. Graner: *J. Theor. Biol.* **164** (1993) 455.
- [56] A. J. Kabla: *J. R. Soc. Interface* **9** (2012) 3268.
- [57] J. A. Glazier and F. Graner: *Phys. Rev. E* **47** (1993) 2128.
- [58] K. Matsushita: *Phys. Rev. E.* **95** (2017) 032415.
- [59] T. E. Angelini, E. Hannezo, X. Trepap, M. Marquez, J. J. Fredberg, and D. A. Weitz: *Proc* **108** (2011) 4714.
- [60] C. Bechinger, R. D. Leonardo, H. Löwen, C. Reichhardt, G. Volpe, and G. Volpe: *Rev. Mod. Phys* **88** (2016) 045006.

- [61] The connection from cells to the self-propelled disks with the continuous change in the shape rigidity is unknown. The simple rigid-limit of these model cells does not correspond to the self-propelled disks because the rigid cells lose propulsion based on the shape deformation. Therefore, the solution of this problem is outside the scope of our model and needs other suitable model.
- [62] A. M. Menzel and T. Ohta: *Europhys. Lett.* **99** (2012) 58001.
- [63] J. T. Bonner: *The Social Amoebae: The Biology of Cellular Slime Molds* (Princeton University Press, Princeton, 2009).